

Study of typical space wave-particle coupling events possibly related with seismic activity

Zhenxia Zhang,¹ ChenYu Wang,² Xuhui Shen,³ Xinqiao Li,⁴ Shugui Wu,¹

Abstract. Based on the DEMETER satellite, we found two space wave-particle coupling events during February 2010 taking place in the range of McIlwain parameter $L(1.27 \sim 1.37)$. There are strong spatial and temporal correlation between the particle bursts(PBs) and the electromagnetic disturbances of the coupling events. The two PBs show different energy spectrum characteristics, while the corresponding electromagnetic disturbances concentrated on different frequencies range. In agreement with the prediction of the theory of wave-particle interaction, we conclude that the two wave-particle interactions can be probably explained as following: one is electron dominant precipitation with energy of $0.09 \sim 0.2$ MeV induced by VLF electromagnetic wave with the frequency of $14 \sim 20$ kHz, and another is proton dominant precipitation with energy of $0.65 \sim 2.85$ MeV induced by VLF electromagnetic wave with the frequency of ≤ 100 Hz. For the first time, those particle bursts origin, from electron or proton detected by the Instrument for the Detection of Particles(IDP) on board, is inferred by theory calculation, although the Instrument has no ability to identify the particle species.

1. Introduction

There are many factors that caused the high energy particle acceleration, precipitation and short-term, sharp particle counting rates increase(particle bursts, or PBs), consisting of ground-based VLF EM transmitter, lightning and thunderstorm, ground nuclear test and blast, seismic activity, volcano natural hazard and so on. The main mechanism is that the EM wave, radiated from those events, couples with the energetic particle in the radiation belt by wave-particle interaction. The interaction accelerates the particle by changing the momentum of the particle, or scatters the pitch angle of the particle and make them enter the bounce or drift loss cone. So that a mass of energetic particle accumulate at certain McIlwain parameter L value to induce the particle precipitation, loss or particle burst.

Many effects of electron belts induced by man-made VLF ground-based transmitters obey the theoretical model of wave-particle interaction. Earlier, Inan *et al.* applied a test-particle model of the gyroresonant wave-particle interaction for calculating the precipitation characteristics of the particle flux by a VLF transmitter(Inan *et al.* [1985]). They found the precipitation of the particle is controlled by the pitch angle distribution near the edge of the loss cone. Horne *et al.*(Horne *et al.* [2005]) studied the mechanism of electron acceleration by wave in the outer radiation belt. They show that the electrons could be accelerated by electromagnetic waves at frequencies of a few kHz, which can also increase the electron flux by more than three orders of magnitude over the observed timescale of one to two days. Based on DEMETER(Detection of Electro-Magnetic

Emissions Transmitted from Earthquake Regions) satellite, Sauvaud and Maggiolo observed enhancements in the 100-600keV drift-loss cone electron fluxes at L values between $1.4 \sim 1.7$ induced by NWC transmitter(Sauvaud and Maggiolo [2008]). They calculated the variation of the energy of enhanced electron fluxes with L by first-order cyclotron resonance theory of wave-particle interaction and obtained consistent results with the observation. Graf *et al.* analyzed the energetic electron flux increase near loss cone induced by ground-based VLF transmissions of NPM observed via satellite-based detection, and compared the precipitating flux with predictions based on ray-tracing analyses of wave propagation and wave-particle interaction(Graf *et al.* [2009]). They indicated that the detection rate is attributed to the orientation of the DEMETER particle detector and obtained the agreement between the observations and theory. Wang *et al.* explained the relationship between the radiation belt electron precipitation observed by DEMETER and the man-made VLF signals in the NPM experiment by the theory of quasi-linear diffusion with resonant interaction, and indicated that most of the non-correlation is caused by the restriction of the pitch angle measurement of IDP (Wang *et al.* [2011]). Li *et al.* analyzed the energy spectrum of the NWC electron belts in detail using on-off method and explained the pitch angle range observed by quasi-linear diffusion equation of wave-particle theory(Li *et al.* [2012]). The illustrations of precipitation of inner radiation belt electrons, induced by VLF transmitters and their explanation by wave-particle interaction, are also included in the work of Inan *et al.*(Inan *et al.* [2007]).

In addition to the man-made VLF transmitter, there are many observations about the energetic electron precipitation and particle bursts caused by seismic activity, observed by satellite detectors. The representative works in this subject includes the correlation between energetic particle burst and seismic activity based on MARIA experiment studied by the papers(Voronov *et al.* [1987, 1989]; Parrot [2009]). Fidani and Battistion performed a detailed analysis to the short-term and sharp increases in high energy particle counting rates and their correlations to seismic activity based on the whole period of ten years burst activity from NOAA data (Fidani and Battistion [2008]).

The DEMETER satellite with a 700 km altitude, 98.3° inclination orbit (Parrot [2006]) serves from June 2004 to

¹National Earthquake Infrastructure Service, China Earthquake Administration, Beijing, China. (zxzhang@neis.gov.cn).

²Peking University, Beijing, China.

³Institute of Earthquake Science, China Earthquake Administration, Beijing, China.

⁴Institute of High Energy Physics, Chinese Academy of Sciences, Beijing, China.

December 2012. An onboard instrument for particle detection (IDP) (Sawvaud *et al.* [2006]) measures 72.9keV~2.35MeV electrons with 8.9 keV resolution in burst mode at one sample per second, and the electric field instrument (ICE) measures electric field fluctuations of 0 ~ 20kHz in burst mode. Based on the credible measurement of electric field and energetic particle flux, we can study the particle precipitation and particle burst events and the wave-particle interaction between them and the VLF waves in detail.

When we look for the ionosphere disturbance in link of Chile Earthquake on 27th February 2010, we found two particle burst events and the corresponding electric field disturbance occurring over epicenter based on Satellite observation (Zhang *et al.* [2012]), with the figures shown in Figure 1 and 2. The energy spectra of the PBs exhibits different distribution structure for the two PBs. In this paper, by calculating the quasi-linear diffusion coefficients for field-aligned electromagnetic waves, we analyze qualitatively the coupling properties of the two PBs and the corresponding

VLF electric spectrum disturbance according to the information of their pitch angle, energy spectrum and frequency range and so on.

2. Observations

The DEMETER satellite, with quasi-Sun-synchronous orbit, flies downward (from north to south) during local daytime and flies upward (from south to north) during local nighttime. The orbital period is 102.86 minutes. Here we select the satellite data of upward orbit to perform statistical analysis as the electromagnetic wave can transmit into the ionosphere in night more easier. We analyzed the high energy particle flux data sample detected by IDP in the first three months of 2010. The charged particle counting rates were considered in three energy regions, 90~600keV, 600~1000keV and 1000~2350keV, respectively. We selected the satellites orbits which fly over the epicenter region (71°00'W, 30°00'S) within the longitude range of 10 degree and L value of 0.1. So there are total 42 orbits across epicenter region of Chile earthquake during seismic activity in the first three months of 2010. Each orbit can fly across the epicenter region in about several minutes.

In Figure. 1, plot (a) displays the distribution of high energy charged particle average counting rates in 2010 (Zhang *et al.* [2012]), from which we can see the peak of the average counting rates very clearly shown on 16th, February in the lower energy region of 90~600keV, named PB1, coming from upward orbits data of 30109. The distribution of the flux enhancement of the PBs with two times flux over the averaged value of background is shown in plot (b). The selected criteria is: $signal/BG \geq 2$, in which signal denotes the real flux in every pixels and BG denotes the averaged value of flux of all revisit orbits in the first three months of year 2010 over the same focus region. The disturbance of the electric field in ionosphere over the same region in the same orbit number 30109 detected by the DEMETER satellite is shown in plot (c). In Figure. 2, we present the the distribution of high energy charged particle average counting rates from the orbit number 30094, the position distribution of the flux enhancement, and the corresponding disturbance of the electric field in ionosphere over the same region with the same orbit number 30094. The peak of the average counting rates appear in energy channel of 600~1000keV and 1000~2350keV from upward orbits data, which is named PB2.

Both two PBs for different energy channels exceed about 4 to 6 times over the average value of the counting rates. The obvious particle counting rates enhancement also appear in the northern hemisphere mirror points conjugate of epicenter, induced by the bounce motion of particles between north and south pole along the geomagnetic field line.

Corresponding to 30109 orbit on 15th February, the frequency range of the electric field disturbance is around 14 to 20 kHz, and corresponding to 30094 orbit on 16th February, the frequency range of the disturbance is less than 100Hz.

Table. 2 show the observation time contrast for the PBs and the VLF electric enhancements. From this table, we can easily find there exists strong temporal correlation between the energetic particle bursts and the VLF electric field disturbance, so they are likely to origin from the same VLF EM source, then the wave-particle interaction takes place in ionosphere at the altitude of DEMETER satellite.

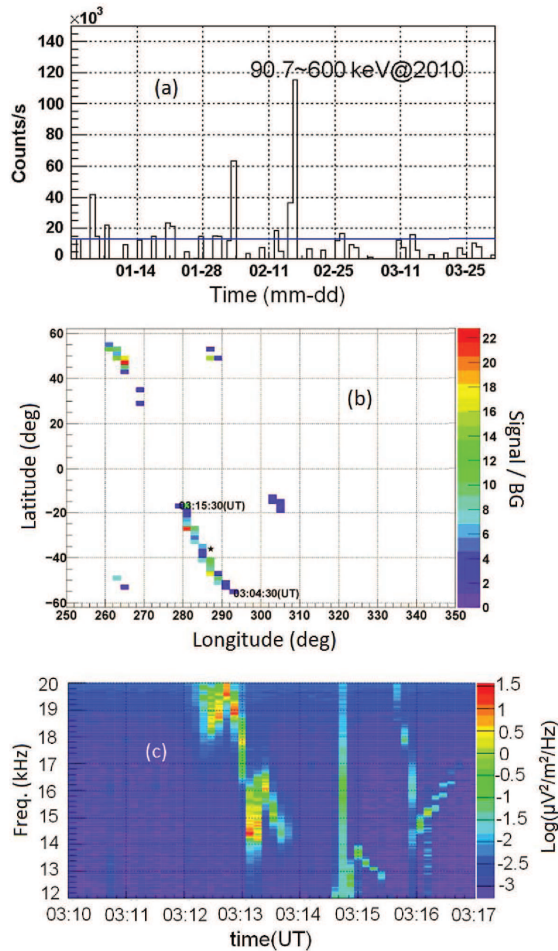


Figure 1. All observed figures for PB1 from orbit 30109 orbit on 16th February. (a) The distribution of averaged high energy charged particle counting rates in 2010. (b) The distribution of position and the duration UT of the energetic particle burst in which the value of Signal over average background is equal or larger than 2. The black star denotes the position of the epicenter of Chile Earthquake. (c) The disturbance of the VLF electric spectrum in ionosphere over the epicenter detected by the DEMETER satellite from the same orbit 30109.

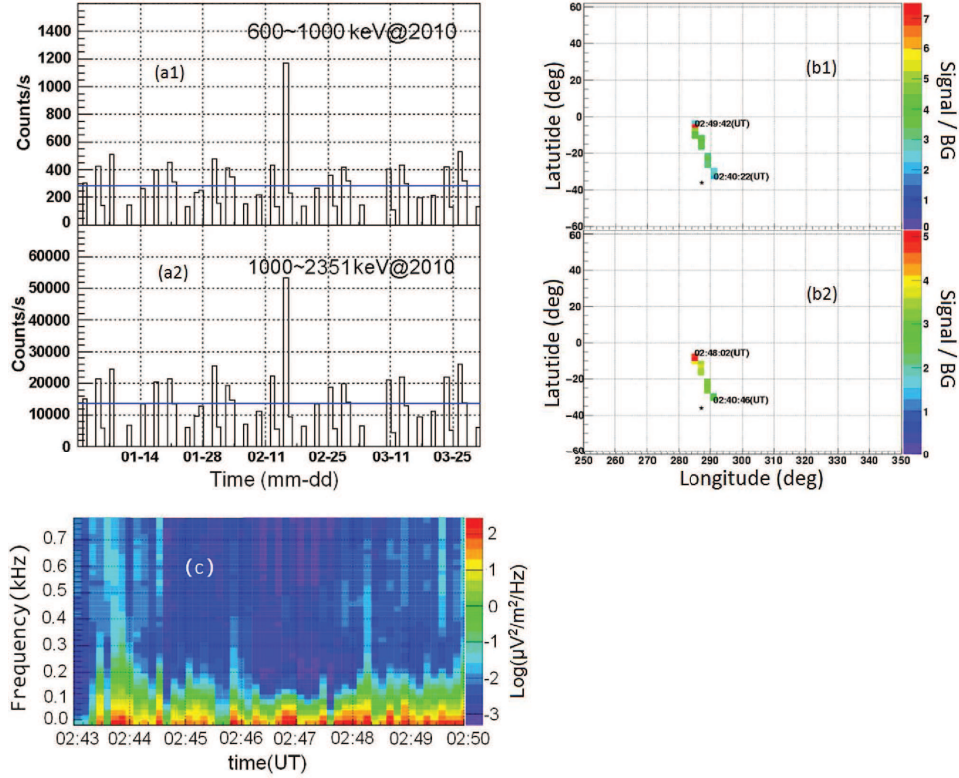


Figure 2. All observed figures for PB2 from orbit 30094 orbit on 15th February. Plots of (a1) and (a2) denotes the distribution of averaged high energy charged particle counting rates. Plots of (b1) and (b2) denotes the distribution of position and the duration UT of the energetic particle burst, for $600 \sim 1000\text{keV}$ and $1000 \sim 2351\text{keV}$ energy channels respectively, in which the value of Signal over average background is equal or larger than 2. The black star denotes the position of the epicenter of Chile Earthquake. (c) The disturbance of the VLF electric spectrum in ionosphere over the epicenter detected by the DEMETER satellite from the same orbit 30094.

Table 1. The parameters contrast of high energy particle bursts and the corresponding VLF electric distribution(VLF). Here the pitch angle denotes the equatorial pitch angle of two PBs. PB1 denotes particle burst from 30109 orbit, PB2 denotes that from 30094 orbit.

event	energy/frequency	time(UT)	time(UT)	Pitch Angle($^{\circ}$)
PB1	90-200keV		03:04:30-03:15:30	21.1-29.8
PB2	150-1000keV	02:40:22-02:49:42		21.4-30.1
PB2	1-2.35MeV	02:40:46-02:48:02		21.4-30.1
VLF1	< 100Hz	02:43:42-02:50:00		
VLF2	14-20kHz		03:12:00-03:14:00	

3. Spectrum of PBs

In order to study the energy spectrum characteristic of the PBs described above, we select the data sample in the first three months of year 2010 over the epicenter region of Chile EQ eliminating the data of 30109 and 30094 orbits, then take it as the background data and compare the energy spectrum of the PBs to the background, shown in Figure. 3.

From the energy spectrum profile, it can be confirmed that the energy of particle counting rates enhancement from 30109 orbit focus on $0.09 \sim 0.2\text{MeV}$, and that from 30094 orbit focus on $0.15 \sim 2.35\text{MeV}$. While the corresponding VLF electric spectrum disturbances coming from the same orbits to the PBs have the EM frequency of $14 \sim 20\text{kHz}$ and less than 100Hz , respectively. The details are concluded in the Table. 2.

There are very big difference for the frequency of VLF wave in the wave-particle interaction between the two cou-

plings, one distributes in $14\text{-}20\text{kHz}$, another in less than 100Hz . Under the same condition of the L value, the equatorial pitch angle, the longitude and latitude and so on, there must be a certain mechanism driving the coupling process, for instance, the two PBs may origin from different particle species: electron and proton. IDP has no ability to identify the particle species, so we have to verify this assumption by theory calculation.

Since the detected electron efficiency is very low in the energy range larger than 1MeV , we assume that the particles of PB2 are likely to coming from the protons. This supposition is proved to be correct in the theory calculation analysis in the next section. The science data of level-1 was reconstructed in the condition of thinking all the particles as electrons, so we need recalculate the incident energy spectrum for the PB2 particles by taking them as protons. In IDP the optic has an aluminum foil with a thickness of $6\mu\text{m}$

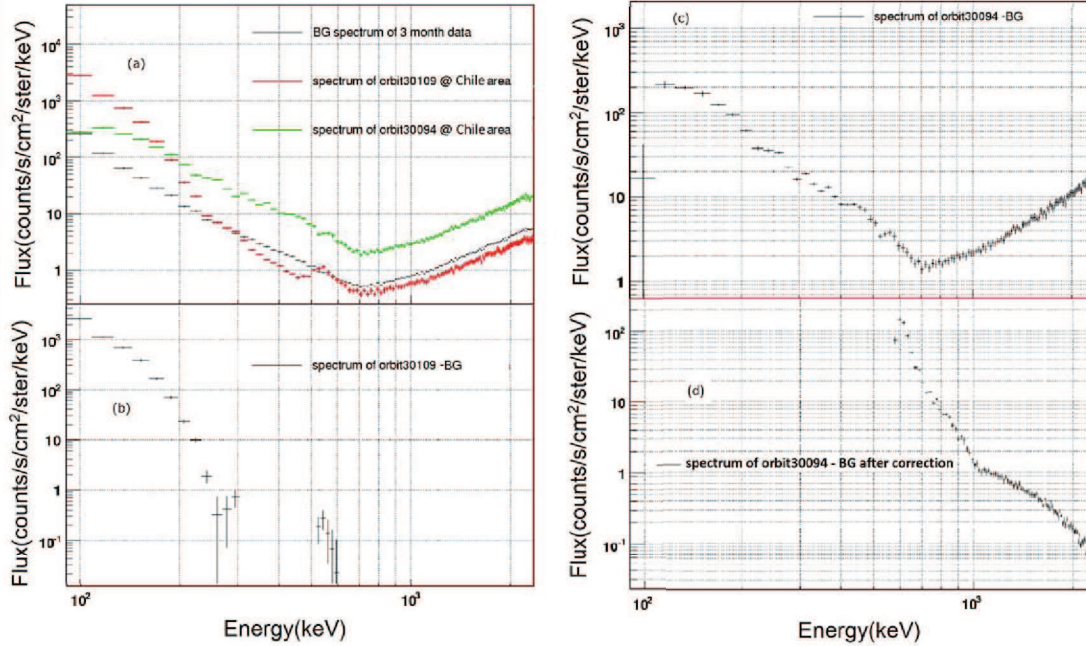


Figure 3. Energy spectrum of PBs and their background. (a) The black profile graph with error bar denotes the average energy spectrum for the first three months of 2010 except that of 15th and 16th February, and the red one for that of 16th February (30109 orbit), the green one for 15th February (30094 orbit). (b) Energy spectrum of PB1 from 30109 subtracting that of background. (c) Energy spectrum of PB2 from 30094 subtracting that of background. (d) Energy spectrum of PB2 from 30094 subtracting that of background, after performing the corrections of efficiency and incident-deposition energy relation of proton.

to stop protons with energies lower than 500keV (Sauvaud *et al.* [2006]). The detected energy spectrum can be derived by counting for the electron efficiency profile. The detected energy spectrum is the same as the incident energy spectrum of proton, since the efficiency of proton penetrating through the aluminum foil is about 100%. So the corrected incident energy range for the particles in PB2 is derived to be 0.65 ~ 2.85 MeV, shown in Figure. 3(d).

IDP has no angular identification ability to the incident particles, but fortunately they recorded the pitch angle by calculating the direction between the axis of IDP aperture and the local magnetic field magnetic field. The pitch angle

for the PBs observed here are presented in Figure. 4. The particle pitch angles are distributed within $76^\circ \sim 78^\circ$ and $80^\circ \sim 82^\circ$ for the two PBs respectively (see Table. 2 for details). At the latitude of $32.8^\circ \sim 39.8^\circ$ corresponding to the selected region above Chile earthquake, the equatorial pitch angles are derived to be: $21.1^\circ \sim 29.8^\circ$ and $21.4^\circ \sim 30.1^\circ$.

4. Verification of Pitch Angle Diffusion Equation in Wave-Particle Interaction Theory

Despite the magnetospheric physics has been studied for more than 40 years, the dynamics of the Earth's particle radiation belts are not well understood and has been attracting people's interest to research it. Among many papers discussing the processes governing the transportation, acceleration, and loss of radiation belt electrons, what engage people's attention is the paper (Gendrin [2001]; Horne [2002]) which assesses the influence of wave-particle interactions on radiation belt electron dynamics. In the early work (Kerner and Petschek [1966]) on pitch angle scattering of radiation belt particles, the gyroresonant wave-particle interaction was thought of playing a crucial role in magnetospheric physics. The work of Summers (Summers [2005]) develops a special form of the quasi-linear diffusion coefficients corresponding to (R-mode or L-mode) electromagnetic waves with a Gaussian spectral density propagating in a hydrogen plasma. They derived a collisionless Vlasov equation for the particle distribution function to the second order in perturbation and obtained the diffusion equation. In the inner radiation belts, the particle velocities generally are much larger than typical phase velocities of waves, so pitch angle diffusion plays a dominant role in the wave-particle interaction.

Originating from the Fokker-Planck equation (Melrose [1980]), the quasi-linear diffusion equation with only pitch-angle diffusion coefficients for cyclotron resonant interaction

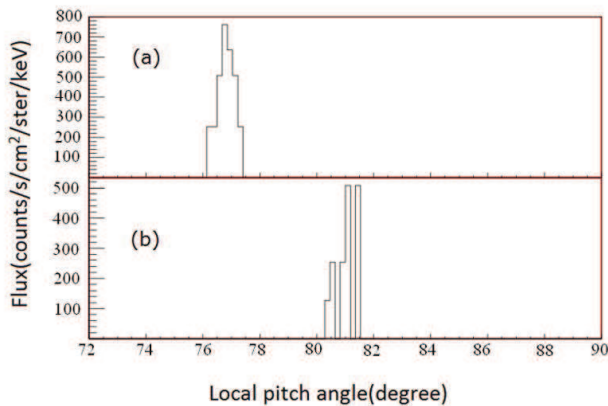


Figure 4. The local pitch angle distribution of the PBs. (a) for PB1 from 30109 orbit, (b) for PB2 from 30094 orbit.

with field-aligned electromagnetic waves of arbitrary spectral density can be written as:

$$\frac{\partial f}{\partial t} = \frac{1}{\sin \alpha} \frac{\partial}{\partial \alpha} (D_{\alpha\alpha} \sin \alpha \frac{\partial f}{\partial \alpha}), \quad (1)$$

where, for one particle of certain species σ , charge q and rest mass m_σ , $f(\alpha, E, L)$ is the density function in the gyrophase-averaged phase space, which depends on the equatorial pitch angle α , the kinetic energy E , and the McIlwain parameter L .

Assuming the wave frequency spectrum density obeys Gaussian distribution, the local pitch angle diffusion coef-

ficient of wave-particle interaction is deduced as following:

$$D_{\alpha\alpha} = \frac{\pi}{2} \frac{1}{\nu} \frac{\Omega_\sigma^2}{|\Omega_e|} \frac{1}{(E+1)^2} \sum_s \sum_j \frac{R(1 - \frac{x \cos \alpha}{y\beta})^2 |F(x, y)|}{\delta x |\beta \cos \alpha - F(x, y)|} \cdot e^{-\left(\frac{x-x_m}{\delta x}\right)^2}, \quad (2)$$

where E is the dimensionless particle kinetic energy given by $E = E_k/(m_\sigma c^2) = \gamma - 1$; $\beta = v/c = [E(E+2)]^{1/2}/(E+1)$; B is the Earth's magnetic field and $R = |\delta B_s|^2/B_0^2$ is the ratio of the energy density of the turbulent magnetic field to that of the background field. $x_m = \omega_m/|\Omega_e|$, $\delta x = \delta\omega/|\Omega_e|$, $s=1$ for R-mode wave and $s=-1$ for L-mode wave. $j = 1, 2, \dots, N$ is the root number of satisfying the resonance condition,

$$\omega_j - \nu \cos \alpha k_j = -s \frac{q}{|q|} \frac{|\Omega_\sigma|}{\gamma}, \quad (3)$$

$F(x, y) = dx/dy$ ($x = \omega/|\Omega_e|$, $y = ck_i/|\Omega_e|$) is determined from the dispersion equation of electron or proton as following:

$$\left(\frac{ck}{\omega}\right)^2 = 1 - \frac{(1+\epsilon)/\alpha^*}{(\omega/|\Omega_e| - s)(\omega/|\Omega_e| + s\epsilon)}, \quad (4)$$

where

$$\alpha^* = \Omega_e^2/\omega_{pe}^2 \quad (5)$$

is an important cold-plasma parameter; ϵ is the rest mass ratio of electron and proton; $|\Omega_e| = e|B_0|/(m_e c)$ denotes the electron gyrofrequency and $\omega_{pe} = (4\pi N_0 e^2/m_e)^{1/2}$ is the plasma frequency, where N_0 denotes the particle number density in ionosphere at the altitude of Satellite observation.

From the VLF electric spectrum distribution and energy spectrum of PBs, the typical wave-particle interaction takes place in the ionosphere. Furthermore, the coupling energy of particle and the frequency of VLF wave take on specific correlation, as listed in Table. 2.

Assuming the wave-particle interaction occurs only within the equatorial plane, we can calculate the equatorial pitch angle diffusion coefficient for the electron coupling with R-mode electromagnetic wave and the proton coupling with L-mode electromagnetic wave. The parameters are chosen as following: the wave amplitude $\delta b = 10$ pT, the equatorial magnetic field determined by a dipole model $B = 3.11 \times 10^{-5}/L^3$ T. The equatorial plasma density N is equal to $N_0 \times (2/L)^4 \text{ cm}^{-3}$ according to the study (Angerami and Thomas [1964]; Inan et al. [1984]). Due to the location of PBs in the South Atlantic Anomaly where the average particle counting ratio is much larger than other region in ionosphere, we select particle density $N_0 = 18000 \text{ cm}^{-3}$ which is at least reasonable in the magnitude comparing to the satellite detection result. The other parameters used in the theory calculation can be found in every plot.

Eventually, we obtained the nice agreement between the DEMETER observation and the quasi-linear diffusion equation calculation, as long as the PBs of 30109 is explained to origin dominantly from electron and the PBs of 30094 from proton, that is, the electron couples with R-mode EM wave and the proton with L-mode EM wave in the wave-particle interaction mechanism. Figure. 5 show the profile of the equatorial pitch angle diffusion coefficient $D_{\alpha\alpha}$ depending on the pitch angle distribution.

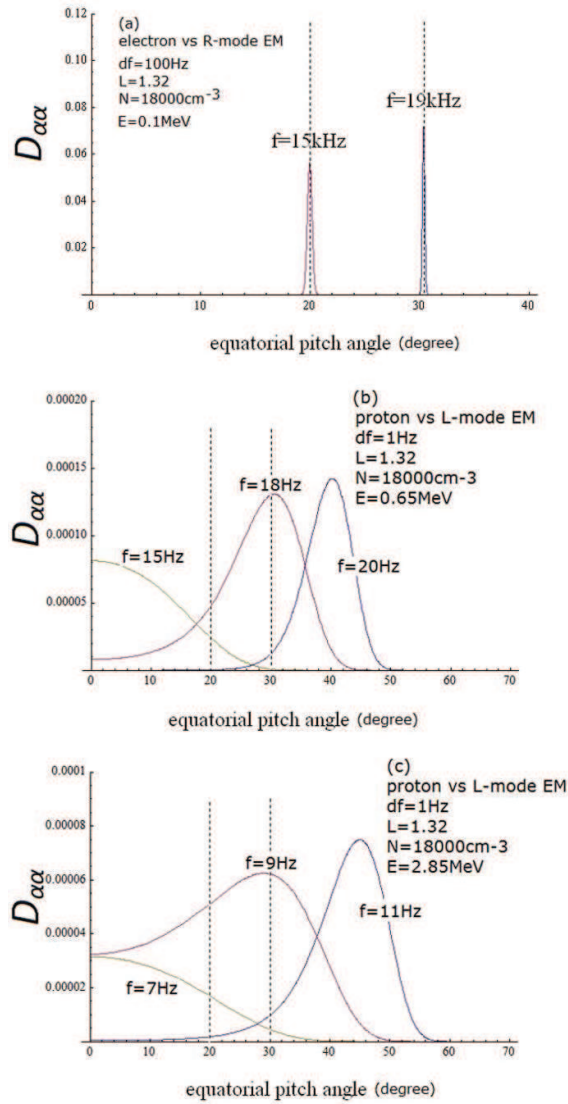


Figure 5. The dependence of pitch angle diffusion coefficient distribution on equatorial pitch angle. The parameters used here are: L value 1.32 and particle density 18000 cm^{-3} . (a) for the electron coupling with R-mode EM wave with the frequency bandwidth 100Hz. (b) for the 0.65MeV proton coupling with L-mode EM wave. (c) for the 2.85MeV proton coupling with L-mode EM wave. The vertical dashed lines denote the satellite observation range in pitch angle.

In Figure. 5, for the coupling of electron and R-mode EM wave, we choose the bandwidth of wave spectrum with $df = 100\text{Hz}$, and for that of proton and L-mode EM wave, the frequency bandwidth is $df=1\text{Hz}$. The L value with $L = 1.32$ in the center of the observation region is selected. The range between two dashed lines in the figure indicates the observation limit of DEMETER satellite. We can find the pitch angle of wave-particle interaction with the electron energy 0.1MeV and VLF EM wave frequency from $15 \sim 19\text{kHz}$ distributes in around $20^\circ \sim 30^\circ$ and just enter the sight of IDP. As for the proton vs L-mode EM wave, considering the parameters range of PBs and the VLF EM wave observed, we select several cases with different interaction parameters and calculate the pitch angle diffusion coefficient. The protons with energy 0.65MeV interact with VLF wave with frequency of 15Hz,18Hz,20Hz. And the protons with energy 2.85MeV interact with wave of 7Hz,9Hz,11Hz. Their pitch angle diffusion can completely or partially fall into the observed range of equatorial pitch angle around $20^\circ \sim 30^\circ$ between the two dashed line in the plots.

Under the condition of a given equatorial pitch angle α , EM frequency f and other parameters, the particle energy of the quasi-linear diffusion coefficient theory relies on the L value. The reports showed a decrease in energy with increasing L from cyclotron resonance(*Koons et al.* [1981]; *Chang and Inan* [1983]). In Figure. 6, we present the coupled energy of electron and proton depending on L value by theoretical calculation, (a)and (b) for electron coupling with R-mode EM wave, (c) and (d) for proton coupling with L-mode EM wave. The equatorial pitch angles in (a) and (c) used in the theoretical calculation are selected to be: 20° and 30° in (b)and (d), which is just consistent with the range of observed PBs listed in the Table. 2. We find that, within the range of $L 1.27 \sim 1.37$, the energy of particle calculated corresponding to the shadow region in each plot is almost consistent with the energy of the PBs observed by DEMETER, that is ,0.1 \sim 0.2MeV for electron and 0 \sim 3.4MeV for proton.

The relation between the particle energy and the VLF EM wave in the wave-particle interaction are shown in the Figure. 7, derived by the resonance condition (3)and the dispersion equation (4).

For electron coupling with R-mode EM wave, the particles with energy of 0.09MeV-0.15MeV interact with VLF EM wave with the frequency of $12 \sim 20\text{kHz}$. For proton vs L-mode wave, particles with energy of 0.65 \sim 2.85 MeV interact with VLF wave with the frequency of less than 100Hz. This calculation results agree mostly well with the observation range of PBs and VLF electric disturbance, seeing the detail in Table. 2.

5. Discussion and Summary

For the study of the high energy particle counting rates enhancement and VLF electric disturbance observed simultaneously in ionosphere, we analyze the energy spectrum of PBs and show the pitch angle distribution of them and point out that the typical wave-particle interaction take place, which induces the energetic charged particle entering the drift loss cone, causing the particle counting rates enhancement locally in ionosphere. The energy range for the two PBs distributes around 0.09 \sim 0.2MeV and 0.65 \sim 2.85 MeV , but the frequency of VLF wave coupling with particles has much big different values $14 \sim 20\text{kHz}$ and less than 100Hz.

If we regard the particles in PBs as electron and proton respectively, the agreement with observation is obtained by calculation of pitch angle quasi-linear diffusion coefficient equation. We verify the supposition by checking three kinds

of correlation formula: pitch angle diffusion coefficient $D_{\alpha\alpha}$ depending on pitch angle α , the coupled particle energy depending on McIlwain parameter L and the relation between coupled particle energy and VLF wave frequency. So it confirms that the PBs and VLF electric spectrum disturbance are caused by a same VLF EM wave source, and proves that we find one typical wave-particle interaction based on DEMETER satellite.

For the first time, under the inability to identify particle species of IDP on board DEMETER, by wave-particle interaction calculation, we point out the particle bursts origin accurately from electron or proton dominant source. In addition, the PBS and electric spectrum disturbance appearing simultaneously over the Chile EQ epicenter about 10 days before the earthquake, if there is really certain link between the PBs and VLF electric disturbance and seismic activity as argued by the paper(*Zhang et al.* [2012]), then this is also the first time that we obtain the evidence of precursor information of seismic activity, that is, the electron and proton counting rate enhancement in ionosphere simultaneously observed by satellite.

The consistent results with observation also prove the correctness and rationality of the theory of quasi-linear diffusion coefficient equation applying in the particle precipitation and wave-particle interaction analysis in the low orbital satellite observation in ionosphere, in turn. It is worth saying that the errors, associated with the negligence of higher-order resonances, are smaller than inaccuracies associated with uncertainties in the input values for the plasma density and latitudinal distribution of the waves. Although the reasonable assumption have been made, there is still some limitation and a long road to describe precisely the observation for the theory. Such as, the accuracy of the plasma density playing an important role in theory always depend on the more accurate measurement of satellite detection to ionosphere. Many researchers studied the outer radiation dynamics of 2D momentum-pitch-angle diffusion equation of energetic electrons interaction with whistler wave, and the translation process of whistler wave during a little strong geomagnetic activities(*Zheng et al.* [1983]; *Xiao et al.* [2011]; *Su et al.* [2009]), and there are still other related works(*Jiang et al.* [2011]; *Zhang et al.* [2014]) focusing on the property of wave propagation and wave-particle interaction. So we will continue further study based on those works and attempt to perform some quantitative calculation.

Laboratory measurements indicate that rock samples under stress can radiate EM energy in a wideband spectrum, and that light can been observed(*Cress et al.* [1987]). Estimations of the size of the EQ preparation zone are thought to be ranging from 150 km for magnitude 5 EQs to more than 2,500 km for magnitude 8(*Dobrovolsky et al.* [1987]). So if it is true that the seismic activity radiate EM waves and the waves can propagate into the ionosphere and diffuse the energetic particles by wave-particle interaction, then we can monitor the particles change to investigate the seismic activity. So we need to explore the theoretical model to provide the support for this hypothesis.

In this paper, we only perform qualitative analysis for the EM waves coupling with energetic particles in ionosphere. In order to systematically quantitatively research seismic electromagnetic radiation in lithosphere-atmosphere-ionosphere and the caused ionospheric disturbance, in the future we will still apply the proper propagation model of EM wave, such as ray tracing method, for calculating the power reduction of waves and the wave normal angles and fields of whistler mode waves in the ionosphere(*Starks et al.* [2009]; *Tao et al.* [2010]). In the process, we will consider using the parameters more close to the real condition, including more real geomagnetic field model rather than the dipole magnetic field, non-uniform magnetic flux density and more real plasma layer density. In term of wave-particle interaction, we will consider the effect of radial diffusion of particle and

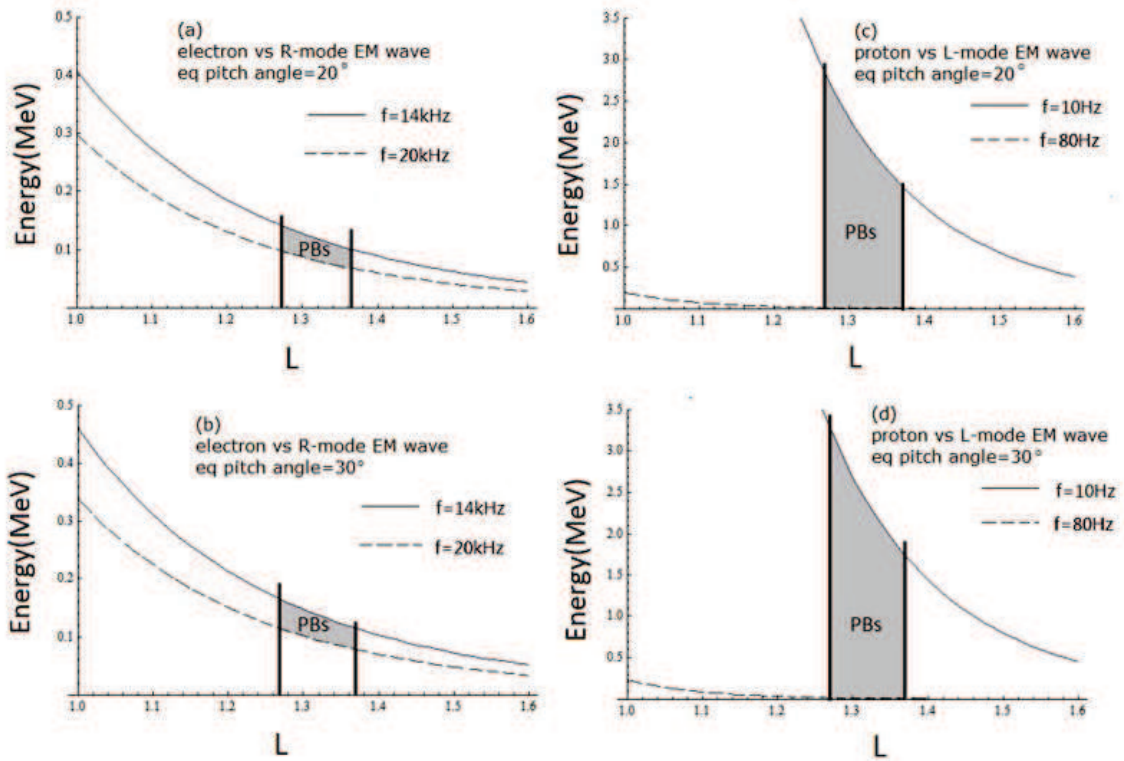


Figure 6. The particle energy calculated by quasi-linear diffusion coefficient equation, shown in the shadow region. Parameter L ranges from 1.27 to 1.37, just in accordance with the range of PBs observed. The solid and dashed curves represent the different wave frequency used in the calculation.

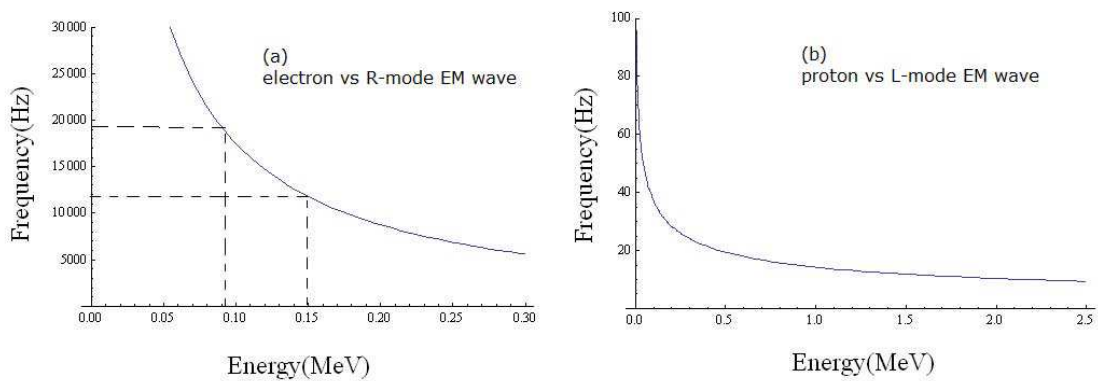


Figure 7. The coupling relation of frequency of EM wave and the energy of particles calculated by the theory of quasi-linear diffusion coefficients, (a) for the electron coupling with R-mode EM wave, (b) for the proton coupling with L-mode EM wave.

apply the non-linear cyclotron resonant interaction of ener-

getic electrons and coherent VLF waves, to quantitatively calculate the precipitation or space distribution change of energetic particles(*Inan et al.* [1978]).

Although the position we select the data to study locates in the South Atlantic Anomaly(SAA), the saturation of IDP detector does not take place. In previous paper(*Zhang et al.* [2012], we show the distribution of high energy charged particle counting rates in the epicenter region for three different energy regions, from left to right plots are the distribution for the year 2007, 2008 and 2009. From these figures, we can find the maximum value of averaged counting rates in the first plot of $90.7 \sim 600\text{keV}$ @2007 is close to 300×10^3 , while the maximum value of the particle burst is only less than 120×10^3 . So there is not saturation of IDP detector above SAA.

The energy spectra in paper(*Zhang et al.* [2012] with the flux increase above 700 keV, does not indicate a pile-up effect of the electronics. The shape of spectra with increase above 700 keV is due to the efficiency correction(*Sauvaud et al.* [2006]). In addition, this case of energy spectrum shape is also the same when the flux is very low. The data we download from DEMETER website is the science data of level-1 after performing efficiency correction. So basically, there is no pile-up for the data we used. The data we used in this work is reliable.

Acknowledgments. The authors would like to express their sincere thanks for the provision of data download of DEMETER Project. This work was supported by Spark Plan for Earthquake Science and Technology of China Earthquake Administration(Grant No XH12066) and National Natural Science Foundation of China(Grant No 11103023) and Director Foundation of National Earthquake Infrastructure Service(2014) .

References

- Inan, U. S., H. C. Chang, and R. A. Helliwell(1985), Precipitation of Radiation Belt Electrons by Man-Made Waves: A Comparison Between Theory and Measurement, *J. Geophys. Res.*, Vol 90, NO. A1, Pages 359-369.
- Horne, R. B., et al. (2005), Wave acceleration of electrons in the Van Allen radiation belts, *Nature*, 437, 227-230, doi:10.1038/nature03939.
- Sauvaud, J.-A., R. Maggiolo, et al.(2008), Radiation belt electron precipitation due to VLF transmitters : satellite observations, *Geophys. Res. Lett.*, 35, L09101, doi:10.1029/2008GL033194.
- Graf, K. L., U. S. Inan, D. Pidtyachiy, P. Kulkarni, M. Parrot, and J. A. Sauvaud(2009), DEMETER observations of transmitter-induced precipitation of inner radiation belt electrons, *J. Geophys. Res.*, VOL 114, A07205, doi:10.1029/2008JA13949.
- Wang, P., et al.(2011), Remediation of radiation belt electrons caused by ground based man-made VLF wave, *Acta Phys.Sin.*, Vol. 60, No. 3, 039401.
- Li, X. Q., et al.(2012), Study of the North West Cape electron belts observed by DEMETER satellite, *J. Geophys. Res.*, Vol. 117, A04201, doi:10.1029/2011JA017121.
- Inan, U. S., M. Golkowski, M. K. Casey, R. C. Moore, W. Peter, P. Kulkarni, P. Kossey, E. Kennedy, S. Meth, and P. Smit, *Geophys. Res. Lett.*(2007), Vol. 34, L02106, doi:10.1029/2006GL028494.
- Voronov, S. A., Galper. A. M., Koldashov, S. V., et al.(1987), Registration of Sporadic Increase of High Energy Particle Flux near Brazilian Anomaly Region, *Proc. of 20th ICRC*, 4, 451-452.
- Voronov, S. A., A. M. Galper, S. V. Koldashov, et al., Observation of high energy charged particle flux increases in SAA region in 10 September 1985, *Cosmic Res.*, 27, 4, 629-631, 1989.
- Parrot, M.(2009), Anomalous seismic phenomena: View from space in Electromagnetic Phenomena Associated with Earthquakes, Ed. by M. Hayakawa, Transworld Research Network, Trivandrum, 205-233.
- Fidani, C. and R. Battistion(2008), Analysis of NOAA particle data and correlations to seismic activity, *Nat. Hazards earth Syst. Sci.*, 8, 1277-1291.
- Parrot, M., et al.(2006), The magnetic field experiments IMSC and its data processing onboard DEMETER: Scientific objectives, description and first results, *Planet. Space Sci.*, 54, 441-455.
- Sauvaud, J. A., T. Moreau, et al.(2006), High-energy electron detection onboard DEMETER: The IDP spectrometer, description and first results on the inner belt, *Planet. Space Sci.*, 54, 502-511, doi:10.1029/2008GL033194.
- Zhang, Z. X., X. Q. Li, et al.(2012), DEMETER satellite observations of energetic particle prior to Chile earthquake. *Chin. J. Geophys.*(in Chinese), 55(5):1581-1590, doi:10.6038/j.issn.0001-5733. 2012. 05. 016.
- Gendrin, R.(2001), The role of wave particle interactions in radiation belts modeling. in *Sun-Earth Connection and Space Weather*, Vol.75, edited by M. Gandini, M. Storini, and U. Villante, P.151, SIF, Bologna.
- Horne, R. B.(2002), The contribution of wave-particle interactions to electron loss and acceleration in the Earth's radiation belts during geomagnetic storms, in *Review of Radio Science 1999-2002*, edited by W.R.Stone, chap.33, pp.801-828, John Wiley, Hoboken, N. J.
- Kernel, C. F. and H. E. Petschek(1966), Limit on stably trapped particle fluxes, *J. Geophys. Res.*, 71, 1.
- Summers, D.(2005), Quasi-linear diffusion coefficients for field-aligned electromagnetic waves with applications to the magnetosphere, *J. Geophys. Res.*, Vol. 110, A08213, doi:10.1029/2005JA011159.
- Melrose, D. B.(1980), *Plasma Astrophysics*, vol. 2, Nonthermal Processes in Diffuse Magnetized Plasmas, Gordon and Breach, New York.
- Angerami, J. J. and J. O. Thomas(1964), Studies of planetary atmospheres: I. The distribution of electrons and ions in the Earth's exosphere, *J. Geophys. Res.*, 69, 4537-4560, doi:10.1029/JZ069i021p04537.
- Inan, U. S., H. C. Chang, R. A. Helliwell(1984), Electron precipitation zones around major ground-based VLF signal sources, *J. Geophys. Res.*, 89, 2891-2906, doi:10.1029/JA089iA05p02891.
- Koons, H. C., B. C. Edgar, and A. L. Vampola(1981), Precipitation of inner zone electrons by Whistler-mode waves from the VLF transmitters UMS and NWC. *J. Geophys. Res.*, 86, 640-648.
- Chang, H. C. and U. S. Inan(1983), Quasi-relativistic electron precipitation due to interactions with coherent VLF waves in the magnetosphere, *J. Geophys. Res.*, 88, 318-328.
- Zheng H N, Su Z P and Xiong M 2008 *Chin. Phys. Lett.* **25**(9) 3515
- Xiao F L, He Z G, Zhang S, Su Z P and Chen L X 2011 *Chin. Phys. Lett.* **28** (3) 039401
- Su Z P, Zheng H N and Xiong M 2009 *Chin. Phys. Lett.* **26** (3) 039401
- Jiang H, Yang X X and Lin M M 2011 *Chin. Phys. B* **20** (1) 019401
- Zhang Z X, Wang C Y, Li Qiang and Wu S G 2014 *Acta. Phys. Sin.* **63** (7) 079401
- Cress G O, Brady B T and Rowell G A 1987 *Geophys. Res. Lett.* **14** 331
- Dobrovolsky I P, Zubkov S I and Miachkin V I 1979 *Pageoph* **117** 1025-1044
- Starks M J, Quinn R A, Ginet G P, Albert J M, Sales G S, Reinisch B W and Song P 2009 *J. Geophys. Res.* **113** A09320
- Tao X, Bortnik J and Friedrich M 2010 *J. Geophys. Res.* **115** A07303
- Inan U S, Bell T F and Helliwell R A 1978 *J. Geophys. Res.* **83** (A7) 3235-3253